INTERNATIONAL JOURNAL FOR NUMERICAL METHODS IN FLUIDS, VOL. 20, 169–185 (1995)

A MULTIBLOCK NAVIER–STOKES ALGORITHM USING EQUAL-ORDER QUADRATIC FINITE ELEMENTS

D. L. HILL* AND E. A. BASKHARONE

Department of Mechanical Engineering, Texas A&M University, College Station, TX 77843-3123, U.S.A.

SUMMARY

A new multiblock pressure-based finite element algorithm has been developed. This methodology implements quadratic interpolation for both the elemental velocity and pressure fields. A direct streamline upwinding scheme previously developed by the authors is used to model the non-linear inertia effects. Details of the algorithm and its multiblock foundation are provided along with validating test cases. The results presented clearly demonstrate the accuracy of this new approach and the differences in the pressure field for an element using quadratic versus the traditional bi linear approximation of the pressure field.

KEY WORDS Finite elements Multiblock Quadratic elements Equal-order

1. INTRODUCTION

Computational fluid dynamics (CFD) algorithms often challenge the CPU/memory limitations of even the most capable supercomputers existing today. The large problem size commonly associated with this type of analysis is principally attributed to the accuracy of the algorithm, the physics of the flow being modelled and the complexity of the flow path geometry. For the same problem a first-order algorithm requires a comparatively more dense computational grid than, say, a third-order scheme to capture the same characteristics of the flow field. Complex flows involving shock waves, multiple shear layers and/or turbulence require a finer grid to resolve the steep gradients in the flow variables. The size of the computational model in terms of element and node counts will also increase with increasing complexity of the flow field. For general flow domains with complex surface geometry more points are needed to accurately represent the shape of the domain boundary segments. All these situations give rise to the need for better CFD algorithms. These algorithms should attempt to reduce the use of computer resources such as in-core memory while increasing the accuracy of the algorithm and the capability to solve larger problems.

The primitive variable segregated approach is a conceptually attractive algorithm for subsonic flows. The basic idea of this algorithm is to sequentially solve for the velocity and pressure on either staggered or non-staggered grids. In this case the intermediate velocity (u^*) is determined from the momentum equations, and the pressure (p) or pressure correction variable (p') is calculated from an

* Formerly with Pratt & Whitney Aircraft, West Palm Beach, FL, U.S.A.

CCC 0271–2091/95/020169–17

Received 27 September 1993
Revised 27 June 1994

equation that is generally obtained by substituting a discretized form of the momentum equation into the continuity equation. This equation is usually Laplacian-like and enforces the conservation of mass. Once the p'-variable is updated, it is used to calculate the correction velocity (u') which is then used to correct the u^*-components. The finite volume community was the first to propose this algorithm methodology and refers to it as the SIMPLE/SIMPLER approach.[1,2]

Adaptation of the SIMPLE/SIMPLER approach to finite elements offers an easy and direct means of simultaneously increasing the accuracy of the solution and the capability to model a complex geometry. The manner in which the pressure or pressure correction equation is formed circumvents the Brabuska–Brezzi compatibility conditions so that equal-order interpolation can be used.[3] Furthermore, this pressure-based approach lends itself to iterative solvers instead of the Gaussian-type solvers typically utilized in the classical Galerkin finite element approaches. This change alone results in a substantial increase in the speed and accuracy in comparison with the classical method.[4]

Segregated finite element algorithms have proven to be a direct extension of the SIMPLE/SIMPLER technology. Benim and Zinser[5] developed such an algorithm based on the SIMPLE technique using two different types of elements. The first was the four-noded element with an additional centre node so that the velocity was interpolated bilinearly and the pressure was assumed constant throughout each element. The other element used was a 'composite' element in which four quadrilateral elements were grouped together. The velocity was still assumed to be bilinear within each element while the pressure field was assumed to be bilinear over the entire group of elements. Advection effects were modelled using modified weighting functions.[6] The final finite element form of the momentum equations used to directly calculate the u^*-velocity was obtained through integration by parts of both the diffusion and pressure gradient terms.[7] As for the p'-equation, relationships between u'-components and p' were derived from the discretized form of the momentum equations. These relationships were then directly inserted into the divergence form of the continuity equation. The resulting form of the p'-equation came out to be Laplacian-like.

The next SIMPLE-like finite element algorithm was reported by Shaw.[8] The element used in this work was a quadrilateral element with bilinear interpolation for both the velocity and pressure. The numerically diffuse quadrature scheme of Hughes was used to model the advection effects.[9] However, in calculating u^*, this algorithm did not invoke integration by parts on the pressure gradient terms in the momentum equations. This new discretized form of the momentum equations was then used to develop the relationships between the velocity and pressure correction terms, namely u'-components and p', respectively. These expressions were inserted into a different form of the continuity equation which was obtained using integration by parts. The resulting form of the p'-equation in this case was also Laplacian-like and was shown to give rise to a symmetric positive definite stiffness matrix. The author reported a slow convergence rate of the p'-equation, a characteristic that is typically associated with the SIMPLE algorithms using finite volume techniques.

The development of a SIMPLER-type approach has been reported by Rice and Schnipke.[10] Their work utilized a quadrilateral element with equal-order interpolation for the velocity and pressure. Advection effects were modelled using a monotone streamline upwind technique.[11] The finite element form of the momentum equations used to calculate u^* was obtained by invoking integration by parts on only the diffusion terms. The absence of u' and p' correction variables for SIMPLER-type algorithms led the authors to develop relationships between the u^*-components and the p-variable from the discretized momentum equations. These expressions were used along with integration by parts on the continuity equation to obtain a true Laplacian-type equation for pressure. Continuity is enforced by substituting the pressure field calculated from this equation back into the discretized momentum equations, thus completing the correction phase of the algorithm.

This current work presents an advanced algorithm based on the reported SIMPLER-type approach. Significant improvements have been realized by unprecedentedly adapting the methodology to be used with eight-noded quadratic elements using equal-order interpolation for the primitive variables. These elements are known to provide an increased accuracy over linear or bilinear elements in existing algorithms. The curve-sided feature of the element adds flexibility and accuracy to the modelling of non-orthogonal domains. The quadratic representation of the elemental pressure variable also increases the rate of convergence for the pressure equation, which in principle will now approach a third-order rate of convergence.[12] This feature has the effect of improving the overall convergence rate of the algorithm.

The current study also incorporates a true multiblock logic which allows the proposed algorithm to model large problems while minimizing computational resources. The concept of a multiblock scheme may generally be viewed as physically breaking up the flow domain into serveral subdomains, solving the resulting subproblems, patching up the solution at the interfaces and resolving the problems towards convergence. In our approach, however, element contributions from all foreign blocks are simultaneously added to the current block being updated. The flow problem in this sense is effectively solved as one continuous problem.

The current multiblock approach differs from the adapting gridding concept but addresses the same class of problems.[13–16] For problems where the flow domain is two-dimensional and stationary in its totality, both approaches can be attractive from different perspectives. However, the multiblock approach is clearly better suited for such engineering problems as rotor/stator interaction. In addition, the development of multiblock technology for three-dimensional problems is a direct extension of the concepts used to develop two-dimensional multiblock algorithms.

2. ANALYSIS

In this section the current algorithm is presented. The starting point for this process consists of stating the governing set of equations valid for a flow field that is Newtonian, steady, incompressible, two-dimensional and laminar:[17]

continuity

$$\frac{\partial u}{\partial x}+\frac{\partial v}{\partial y}=0 \tag{1a}$$

x-momentum

$$\rho u\frac{\partial u}{\partial x}+\rho v\frac{\partial u}{\partial y}=-\frac{\partial p}{\partial x}+\frac{\partial}{\partial x}\left(\mu\frac{\partial u}{\partial x}\right)+\frac{\partial}{\partial y}\left(\mu\frac{\partial u}{\partial y}\right), \tag{1b}$$

y-momentum

$$\rho u\frac{\partial v}{\partial x}+\rho v\frac{\partial v}{\partial y}=-\frac{\partial p}{\partial y}+\frac{\partial}{\partial x}\left(\mu\frac{\partial v}{\partial x}\right)+\frac{\partial}{\partial y}\left(\frac{\partial v}{\partial y}\right), \tag{1}$$

where u, v, p, ρ and μ are the two velocity components, pressure, density and absolute viscosity respectively. Next we define the following group of non-dimensional variables:

$$u^*=\frac{u}{U}, \qquad v^*=\frac{v}{U}, \qquad p^*=\frac{p-P}{\rho U^2}, \qquad x^*=\frac{x}{L}, \qquad y^*=\frac{y}{L}, \tag{2}$$

where U is a reference velocity, L is a reference length and P is a reference pressure. Inserting these relations into equations (1a–c) will produce the equivalent non-dimensional form of the governing equations:

continuity

$$\frac{\partial u^*}{\partial x^*} + \frac{\partial v^*}{\partial y^*} = 0, \tag{3a}$$

x-momentum

$$u^* \frac{\partial u^*}{\partial x^*} + v^* \frac{\partial u^*}{\partial y^*} = -\frac{\partial p^*}{\partial x^*} + \frac{1}{Re}\left(\frac{\partial^2 u^*}{\partial x^{*2}} + \frac{\partial^2 u^*}{\partial y^{*2}}\right), \tag{3b}$$

y-momentum

$$u^* \frac{\partial v^*}{\partial x^*} + v^* \frac{\partial v^*}{\partial y^*} = -\frac{\partial p^*}{\partial y^*} + \frac{1}{Re}\left(\frac{\partial^2 v^*}{\partial x^{*2}} + \frac{\partial^2 v^*}{\partial y^{*2}}\right), \tag{3c}$$

where Re is the Reynolds number defined to be $LU\rho\backslash\mu$. Using equations (3a–c), the general form of the finite element weighted residual equations can now be written directly (note that the superscript asterisks have been dropped in order to simplify the notation):

continuity

$$\int W_i\left(\frac{\partial u}{\partial x} + \frac{\partial v}{\partial y}\right) \mathrm{d}A^e = 0, \tag{4a}$$

x-momentum

$$\int W_i\left(u\frac{\partial u}{\partial x} + v\frac{\partial u}{\partial y}\right) \mathrm{d}A^e = -\int W_i \frac{\partial p}{\partial x} \mathrm{d}A^e + \frac{1}{Re}\int W_i\left(\frac{\partial^2 u}{\partial x^2} + \frac{\partial^2 u}{\partial y^2}\right) \mathrm{d}A^e, \tag{4b}$$

y-momentum

$$\int W_i\left(u\frac{\partial v}{\partial x} + v\frac{\partial v}{\partial y}\right) \mathrm{d}A^e = -\int W_i \frac{\partial p}{\partial y} \mathrm{d}A^e + \frac{1}{Re}\int W_i\left(\frac{\partial^2 v}{\partial x^2} + \frac{\partial^2 v}{\partial y^2}\right) \mathrm{d}A^e, \tag{4c}$$

where W_i is the weighting function and $\mathrm{d}A^e$ is the differential element area. Integration by parts is now performed on the continuity equation and on the diffusion terms in the momentum equations:

continuity

$$\int \frac{\partial W_i}{\partial x} u + \frac{\partial W_i}{\partial y} v \, \mathrm{d}A^e = \int W_i (V \cdot n) \mathrm{d}l, \tag{5a}$$

x-momentum

$$\int W_i\left(u\frac{\partial u}{\partial x} + v\frac{\partial u}{\partial y}\right) \mathrm{d}A^e + \frac{1}{Re}\int \left(\frac{\partial W_i}{\partial x}\frac{\partial u}{\partial x} + \frac{\partial W_i}{\partial y}\frac{\partial u}{\partial y}\right) \mathrm{d}A^e = -\int W_i \frac{\partial p}{\partial x} \mathrm{d}A^e + \frac{1}{Re}\int W_i (\nabla u \cdot n) \mathrm{d}l, \tag{5b}$$

y-momentum

$$\int W_i\left(u\frac{\partial v}{\partial x} + v\frac{\partial v}{\partial y}\right) \mathrm{d}A^e + \frac{1}{Re}\int \left(\frac{\partial W_i}{\partial x}\frac{\partial v}{\partial x} + \frac{\partial W_i}{\partial y}\frac{\partial v}{\partial y}\right) \mathrm{d}A^e = -\int W_i \frac{\partial p}{\partial y} \mathrm{d}A^e + \frac{1}{Re}\int W_i (\nabla v \cdot n) \mathrm{d}l, \tag{5c}$$

where V is the velocity vector, n is the unit normal vector and $\mathrm{d}l$ is the differential length. The resulting line integrals in equations (5b,c) are considered natural boundary conditions that can be evaluated on boundary regions if Dirichlet-type conditions are not possible. Note that for a fully developed flow boundary condition at an exit region these natural boundary conditions are exactly zero, so that no

explicit effort has to be made to impose this condition on the momentum equations. As for the line integral in equation (5a), the need to evaluate this term at any boundary region depends on the pressure specification. In cases where only a pressure 'datum' is used, the integral is evaluated using the most current solution. This integral is also evaluated at any boundary where the velocity profile is specified.

The finite element interpolation expressions of the field variables for the eight-noded element of the Serendipity family (Figure 1) can be written in the general form

$$\begin{aligned} u &= \sum_{j=1}^{8} N_j u_j, \qquad v = \sum_{j=1}^{8} N_j v_j, \qquad p = \sum_{j=1}^{8} N_j p_j, \\ x &= \sum_{j=1}^{8} N_j x_j, \qquad y = \sum_{j=1}^{8} N_j y_j. \end{aligned} \tag{6}$$

Equations (6) and (5b,c) are used to develop the final weighted residual finite element form of the momentum equations as follows

x-momentum

$$\int W_i \left(N_k u_k \frac{\partial N_j}{\partial x} + N_k v_k \frac{\partial N_j}{\partial y} \right) u_j \, \mathrm{d}A^e + \frac{1}{Re} \int \left(\frac{\partial W_i}{\partial x} \frac{\partial N_j}{\partial x} + \frac{\partial W_i}{\partial y} \frac{\partial N_j}{\partial y} \right) u_j \, \mathrm{d}A^e = - \int W_i \frac{\partial N_j}{\partial x} p_j \, \mathrm{d}A^e + \frac{1}{Re} \int W_i (\nabla u \cdot n) \mathrm{d}l, \tag{7a}$$

y-momentum

$$\int W_i \left(N_k u_k \frac{\partial N_j}{\partial x} + N_k v_k \frac{\partial N_j}{\partial y} \right) v_j \, \mathrm{d}A^e + \frac{1}{Re} \int \left(\frac{\partial W_i}{\partial x} \frac{\partial N_j}{\partial x} + \frac{\partial W_i}{\partial y} \frac{\partial N_j}{\partial y} \right) v_j \, \mathrm{d}A^e = - \int W_i \frac{\partial N_j}{\partial y} p_j \, \mathrm{d}A^e + \frac{1}{Re} \int W_i (\nabla v \cdot n) \mathrm{d}l. \tag{7b}$$

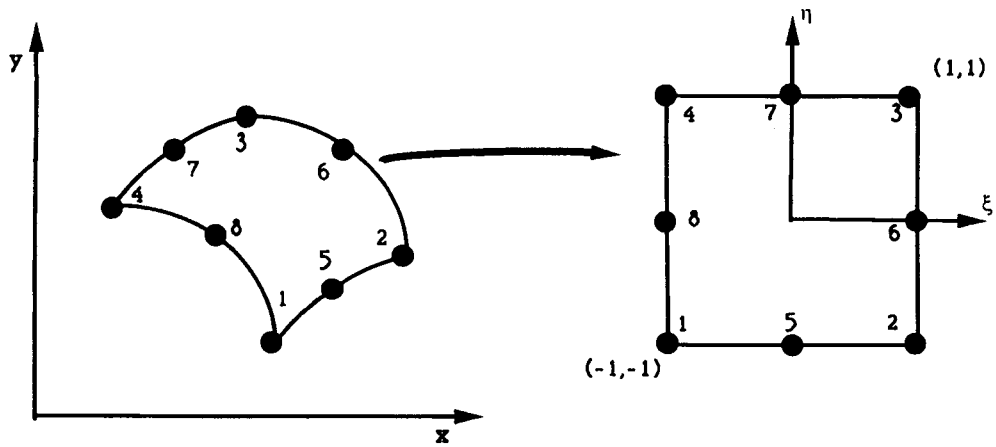

Figure 1. Eight-noded element of Serendipity family.

$$\phi(\eta, \xi) = \sum_{i=1}^{8} \phi_i N_i(\eta, \xi), \quad x(\eta, \xi) = \sum_{i=1}^{8} x_i N_i(\eta, \xi), \quad y(\eta, \xi) = \sum_{i=1}^{8} y_i N_i(\eta, \xi)$$

The current form of the advection terms in equations (7a,b) is the traditional form resulting from the weighted residual approach. This approach is not desirable because it treats these terms in an unrealistic symmetrical manner. Such a representation will cause the algorithm to be driven unstable as *Re* is increased. This behaviour is equivalent to the problems encountered when central differencing is applied to the convection terms. Consequently, these terms are replaced with an upwinding scheme which is based on a direct streamline approach. The accuracy of the method and details of applying it to quadratic elements are given by Hill and Baskharone.[18] The following notation will be used to represent the upwinding technique:

$$u_s \int W_i \frac{\partial u}{\partial s} \, \mathrm{d}A^e = \int W_i \left(N_k u_k \frac{\partial N_j}{\partial y} + N_k v_k \frac{\partial N_j}{\partial y} \right) u_j \, \mathrm{d}A^e, \tag{8a}$$

$$u_s \int W_i \frac{\partial v}{\partial s} \, \mathrm{d}A^e = \int W_i \left(N_k u_k \frac{\partial N_j}{\partial x} + N_k v_k \frac{\partial N_j}{\partial y} \right) v_j \, \mathrm{d}A^e, \tag{8b}$$

where the subscript (s) refers to values along a streamline. Using these relations and choosing the weighting function to be of the same order as the interpolates, the complete finite element form of the momentum equations is obtained:

x-momentum

$$u_s \int N_i \frac{\partial u}{\partial s} \, \mathrm{d}A^e + \frac{1}{Re} \int \left(\frac{\partial N_i}{\partial x} \frac{\partial N_j}{\partial x} + \frac{\partial N_i}{\partial y} \frac{\partial N_j}{\partial y} \right) u_j \, \mathrm{d}A^e = - \int N_i \frac{\partial N_j}{\partial x} p_j \, \mathrm{d}A^e + \frac{1}{Re} \int N_i (\nabla u \cdot n) \mathrm{d}l, \tag{9a}$$

y-momentum

$$u_s \int N_i \frac{\partial v}{\partial s} \, \mathrm{d}A^e + \frac{1}{Re} \int \left(\frac{\partial N_i}{\partial x} \frac{\partial N_j}{\partial x} + \frac{\partial N_i}{\partial y} \frac{\partial N_j}{\partial y} \right) v_j \, \mathrm{d}A^e = - \int N_i \frac{\partial N_j}{\partial y} p_j \, \mathrm{d}A^e + \frac{1}{Re} \int N_i (\nabla v \cdot n) \mathrm{d}l. \tag{9b}$$

Equations (9a,b) are solved first in the interation sequence. The resulting velocities are referred to as the intermediate velocity field. This velocity field has to be corrected by a pressure closure to impose the global conservation of mass.

The pressure equation is developed by substituting a semidiscretized form of the momentum equations into the continuity equation (5a):

x-momentum

$$a_{ii} u_i + \sum_{j=1,m}^{i \neq j} a_{ij} u_j = - \int N_i \frac{\partial p}{\partial x} \mathrm{d}A^e + s_i^u, \tag{10a}$$

y-momentum

$$a_{ii} v_i + \sum_{j=1,m}^{i \neq j} a_{ij} v_j = - \int N_i \frac{\partial p}{\partial y} \mathrm{d}A^e + s_i^v, \tag{10b}$$

where a_{ii} is the diagonal coefficient of the global matrix for row i, a_{ij} refers to the off-diagonal coefficients of the global matrix for row i, m is the total number of positions in row i, and s_i is a source term. Equations (10a,b) are the discretized form of equations (9a,b) but with the pressure gradient in the form given by equations (5b,c). These equations imply that the pressure gradient at a given node is known. Next equations (10a,b) are manipulated to obtain explicit

expressions for the nodal velocity components:

$$u_i = \hat{u}_i - K_u \frac{\partial p}{\partial x}, \tag{11a}$$

$$v_i = \hat{v}_i - K_v \frac{\partial p}{\partial y}, \tag{11b}$$

where

$$\hat{u}_i = \frac{1}{a_{ii}} \left(- \sum_{j=1,m}^{i \neq j} a_{ij} u_j + s_i^u \right), \qquad K_u = \frac{1}{a_{ii}} \int N_i \, \mathrm{d}A^e,$$

$$\hat{v}_i = \frac{1}{a_{ii}} \left(- \sum_{j=1,m}^{i \neq j} a_{ij} v_j + s_i^s \right), \qquad K_v = \frac{1}{a_{ii}} \int N_i \, \mathrm{d}A^e.$$

Equations (11a,b) are now inserted into equation (5a) to obtain the relation

$$\int \frac{\partial N_i}{\partial x} \left(\hat{u} - K_u \frac{\partial p}{\partial x} \right) + \frac{\partial N_i}{\partial y} \left(\hat{v} - K_v \frac{\partial p}{\partial y} \right) \mathrm{d}A^e = \int N_i (V \cdot n) \mathrm{d}l.$$

In order to complete the pressure equation, the pressure gradient is now assumed to be unknown and $\hat{u}$, K_u, $\hat{v}$, and K_v are considered to be nodal quantities. The final form is given below:

$$\int \left(N_k K_{uk} \frac{\partial N_i}{\partial x} \frac{\partial N_j}{\partial x} + N_k K_{vk} \frac{\partial N_i}{\partial y} \frac{\partial N_j}{\partial y} \right) p_j \, \mathrm{d}A^e = \int \frac{\partial N_i}{\partial x} (N_k \hat{u}_k) + \frac{\partial N_i}{\partial y} (N_k \hat{v}_k) \, \mathrm{d}A^e + \int N_i (V \cdot n) \mathrm{d}l. \tag{12}$$

Note that the resulting form of the pressure equation is truly Laplacian and will provide a positive definite symmetric global matrix.

In the current algorithm the updated pressure field obtained from equation (12) is used to correct the intermediate velocity. The discretized momentum equations obtained from equations (9a,b) are used for this final step in the iteration loop. This gives rise to the nodal velocity correction expressions.

$$u_i = \hat{u}_i + \frac{1}{a_{ii}} \sum_{j=1,m} b_{ij}^u p_j, \tag{13a}$$

$$v_i = \hat{v}_i + \frac{1}{a_{ii}} \sum_{j=1,m} b_{ij}^v p_j, \tag{13b}$$

where b_{ij} is an entry in the global matrix from the momentum equations for pressure. This matrix is obtained by integrating the appropriate derivatives of the weighting functions and summing contributions over all elements. The use of equations (13a,b) for the velocity correction step is attractive, because no matrix inversions are required.

The general iteration sequence begins by evaluating equations (9a,b) for the intermediate velocity. Next equation (12) is evaluated to update the pressure field. The sequence is completed when equations (13a,b) are used to correct the intermediate velocity field.

The efficient use of quadratic elements with this algorithm requires the characteristics of the interpolation functions to be adapted to the algorithm. It is desirable that the assembled nodal values obtained by integrating the interpolation function associated with a given node over all elements will be either all positive or all negative values for internal nodes in the computational domain. There are principally two places in the algorithm where the integral of the weighting function is used. The first place is in the upwinding scheme and the second is in the pressure equation. The sign pattern of the assembled nodal values obtained from integration of the quadratic functions will be 'plus', 'minus',

'plus', etc. This characteristic is addressed in the development of the upwinding scheme so that a positive definite matrix will always emerge, allowing the global matrix to be solved by iterative methods.

The alternating sign pattern prohibits the use of an iterative solver for the pressure equation. An LU decomposition method is used instead.[19] The symmetric structure of this equation allows only half of the bandwidth to be stored. No under relaxation is used for this step or when the pressure is updated at the end of an iteration loop. Under relaxation is only used for the calculation of the velocity field.

The basic concept of the multiblock approach is to use a set of finite element models to model a single flow path. The resulting composite solution should approach the flow field corresponding to an equivalent single finite element model of the entire flow path. Implementation of the proposed approach with the current pressure-based algorithm required some modifications to the finite element equations. All interface regions are constructed to have a column or row of nodes that are common to several blocks (Figure 2). The influence of non-active blocks on an active block occurs through these nodes. The new nodal momentum equations valid for any of these common nodes can be written in the following discretized form:

x-momentum

$$(a_{ii} + a'_{ii})u_i + \sum_{j=1,m}^{i\neq j} (a_{ij} + a'_{ij})u_j = \sum_{j=1,m} (b^u_{ij} + b^{u'}_{ij})p_j + s^u_i, \tag{14a}$$

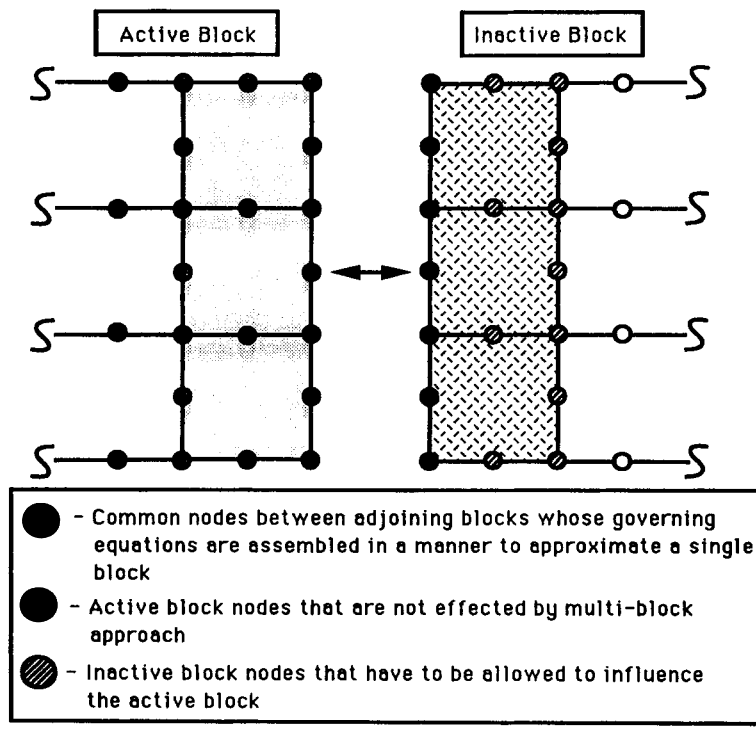

Figure 2. Multiblock approach for finite elements

y-momentum

$$(a_{ii} + a'_{ii})v_i + \sum_{j=1,m}^{i\neq j} (a_{ij} + a'_{ij})v_j = \sum_{j=1,m} (b^v_{ij} + b^{v'}_{ij})p_j + s^v_i, \tag{14b}$$

where

$$s^u_i = \sum_{j=1,k} b^{u'}_{ij} p'_j - \sum_{j=1,k} a'_{ij} u'_j,$$

$$s^v_i = \sum_{j=1,k} b^{v'}_{ij} p'_j - \sum_{j=1,k} a'_{ij} v'_j$$

and the superscript primes denote contributions which are obtained from a foreign block. With these changes in the momentum equations the definitions of $\hat{u}$ and $\hat{v}$ have to be modified. The new forms of these expressions can be written directly from equations (14a,b):

$$\hat{u}_i = -\sum_{j=1,m}^{i\neq j} (a_{ij} + a'_{ij})u_j - \sum_{j=1,k} a'_{ij} u'_j, \tag{15a}$$

$$\hat{v}_i = -\sum_{j=1,m}^{i\neq j} (a_{ij} + a'_{ij})v_j - \sum_{j=1,k} a'_{ij} v'_j. \tag{15b}$$

The changes necessary for the pressure equation can be written in the discretized form

$$(c_{ii} + c'_{ii})p_i + \sum_{j=1,m}^{i\neq j} (c_{ij} + c'_{ij})p_j = d_i - \sum_{j=1,k} c'_{ij} p'_j, \tag{16}$$

where d_i represents the source term generated from the $\hat{u}$ and $\hat{v}$ integral expressions in equation (12).

The last step of the algorithm is the correction phase. The required modifications for this step are given below:

$$u_j = \hat{u}_i - \sum_{j=1,m} (b^u_{ij} + b^{u'}_{ij})p_j - \sum_{j=1,k} b^{u'}_{ij} p'_j, \tag{17a}$$

$$v_i = \hat{v}_i - \sum_{j=1,m} (b^v_{ij} + b^{v'}_{ij})p_j - \sum_{j=1,k} b^{v'}_{ij} p'_j. \tag{17b}$$

Equations (14a,b), (16), and (17a,b) are used to solve for the common nodes between adjoining blocks. It is important to note that there are no natural boundary integrals in these expressions, meaning that these nodes are always treated as internal nodes.

The logic required to control the interface transfer of information was developed using a north/south/east/west notation. This notation along with the structured shape of the finite element models allowed the development of interface routines that can accommodate arbitrary block interface orientations. Once the solution of a region is updated, the calculation and transfer of information as input to other surrounding blocks is handled as a postprocessing task.

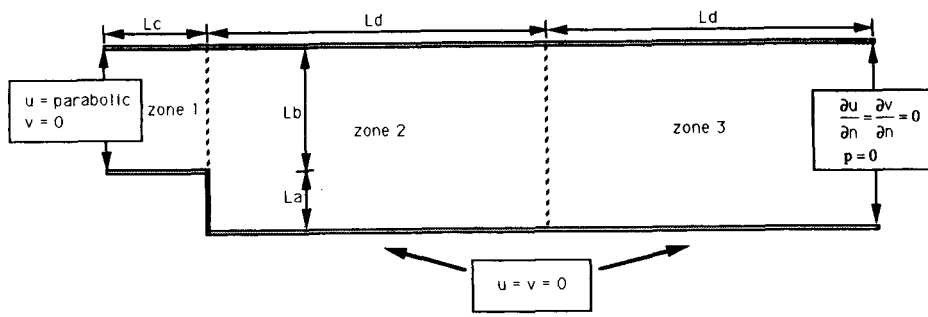

Figure 3. Description of backward-facing step problem $La = 1$, $Lb = 2$, $Lc = 1.33$, $Ld = 8$.

3. RESULTS

The multiblock algorithm was used to analyse the backward-facing step problem depicted in Figure 3. The three blocks shown in this figure have a combined total of 1136 elements. The composite finite element model is shown in Figure 4. No-slip boundary conditions are imposed at all solid walls. A fully developed velocity profile is fixed at the inlet region. For the exit plane, zero-streamwise velocity gradients are assumed and a pressure datum point is arbitrarily given a value of zero.

The streakline trace for the case of $Re = 73$ is shown in Figure 5. No discontinuities can be seen at

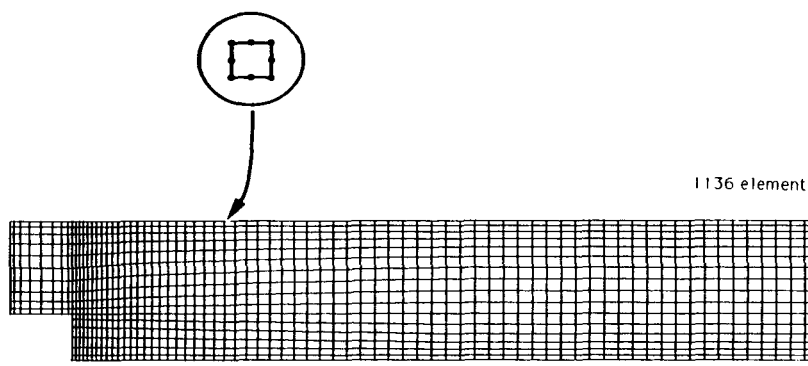

Figure 4. Combined finite element model for backward-facing step problem

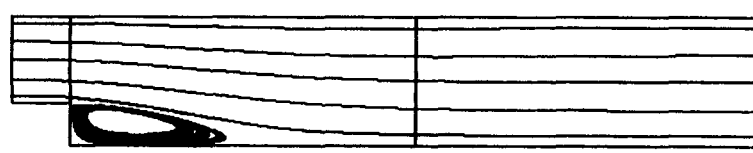

Figure 5. Streakline trace for $Re = 73$

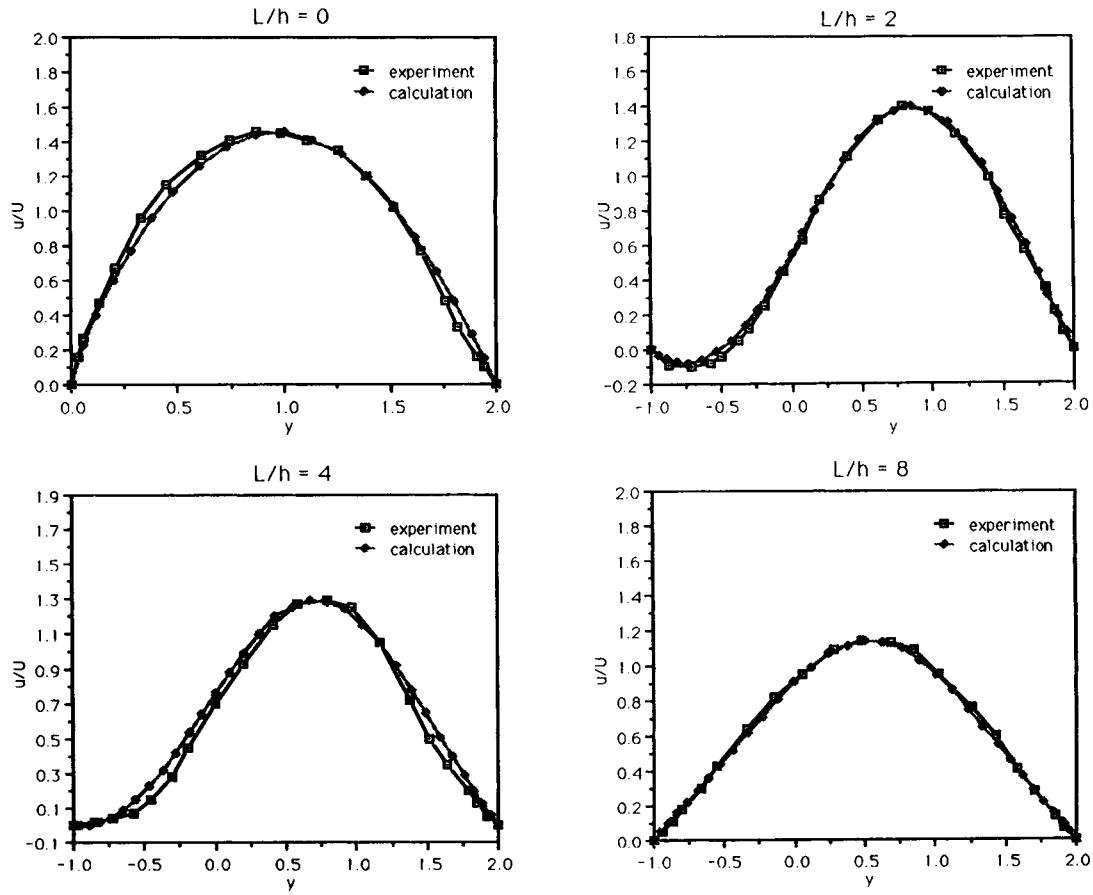

Figure 6. Axial development of velocity profiles for $Re = 73$

any of the interfaces. The axial development of the velocity field for the same Re is compared with the experimental results of Denham and Patrick[20] in Figure 6. The reference starting point ($L/h = 0$) in this case coincides with the step. The comparison clearly shows that the multiblock approach predictions are very realistic. The differences in the velocity profiles can principally be attributed to the three-dimensional effects observed during the experiment.

The contour plot of pressure is shown in Figure 7. Again there are no sharp discontinuities across any interface region. The continuous field shown in this figure is a direct result of the elemental quadratic representation of the pressure variable. The pressure field for the current case was carefully

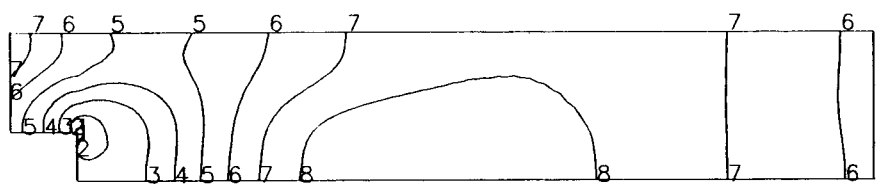

Figure 7. Contour plot of pressure for $Re = 73$. 1, -1.00×10^{-1}; 2, -7.96×10^{-2}; 3, -5.87×10^{-2}; 4, -3.79×10^{-2}; 5, -1.70×10^{-2}; 6, 3.74×10^{-3}; 7, 2.45×10^{-2}; 8, 4.54×10^{-2}

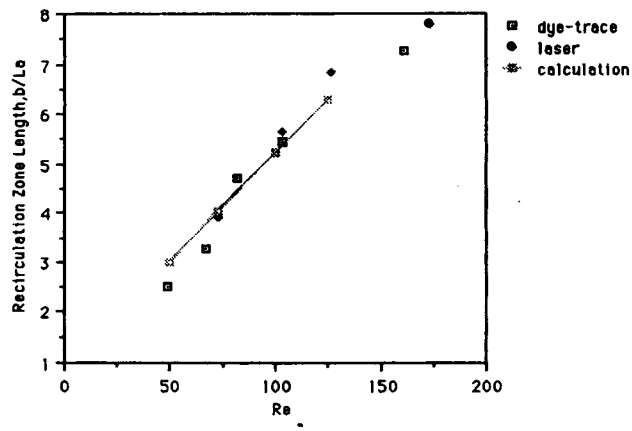

Figure 8. Change in recirculation zone length as a function of *Re*

compared with those presented in References 5, 10 and 21 in which lower-order interpolation was used for the pressure variable. Evidence of a more continuous pressure field was obtained for our case. Again the key contributor was the use of higher-order interpolation for pressure.

The change in the recirculation zone length as a function of *Re* is shown in Figure 8. As *Re* is increased, the length of the recirculation zone also increases. Examination of this figure reveals that the predicted recirculation zone lengths fall within the variations in the reported experimental data.

The next problem considered is a 90° planar branch problem. This type of geometry has a number of applications in the biomedical field. The problem description is given in Figure 9. Two blocks comprising a total of 504 finite elements were used to generate the composite finite element model shown in Figure 10. The no-slip boundary condition for velocity is imposed at all solid boundaries. The inlet region has a fully developed velocity profile. At the exit region, true fully developed flow is assumed. The entire exit plane pressure is set to zero and zero-streamwise velocity gradients are imposed. Physically speaking, both branches in this problem were supposed to discharge the flow to the same back pressure. The difficulty of this bifurcation problem stems from the characteristic that as *Re* is increased, the amount of mass in the principal branching direction is reduced. This means that the amount of mass making the turn is decreased as *Re* is increased.

The streakline traces for *Re* = 50, 200 and 400 are shown in Figures 11–13 respectively. Review of these traces shows that the recirculation zone size increases with increasing *Re*. The larger recirculation zones restrict the amount of mass flow entering the branch. The variation in recirculation zone length with changing *Re* is compared with the prediction of Hayes *et al.*[22] in Figure 14. There are noticeable differences between the two predictions as *Re* is increased. The cause of the differences can be traced back to the length of the branching ducts used in the calculations. The work of Hayes *et al.* implemented a non-dimensional length of 3 while the current analysis used a non-dimensional length of 10. At higher *Re* the shorter-length duct in Hayes *et al.*'s case is viewed as a source of inaccuracy because it does not allow the flow field to develop naturally. Instead the flow field must fictitiously adjust itself to satisfy the fully developed flow constraints at the exit stations. The shorter-length duct would be numerically acceptable if the branching duct width were reduced. The cited work proves this fact by presenting the variation in recirculation zone length as a function of *Re* for cases in which the duct width is 0.75 and 0.5 of the primary duct width. The shapes of the curves for these two cases follow the same trends presented for the current analysis using equal duct width magnitudes.

Figure 15 compares the pressure distribution at *Re* = 200 for the proposed multiblock approach and the classical Galerkin approach using mixed interpolation and a single finite element model (Figure

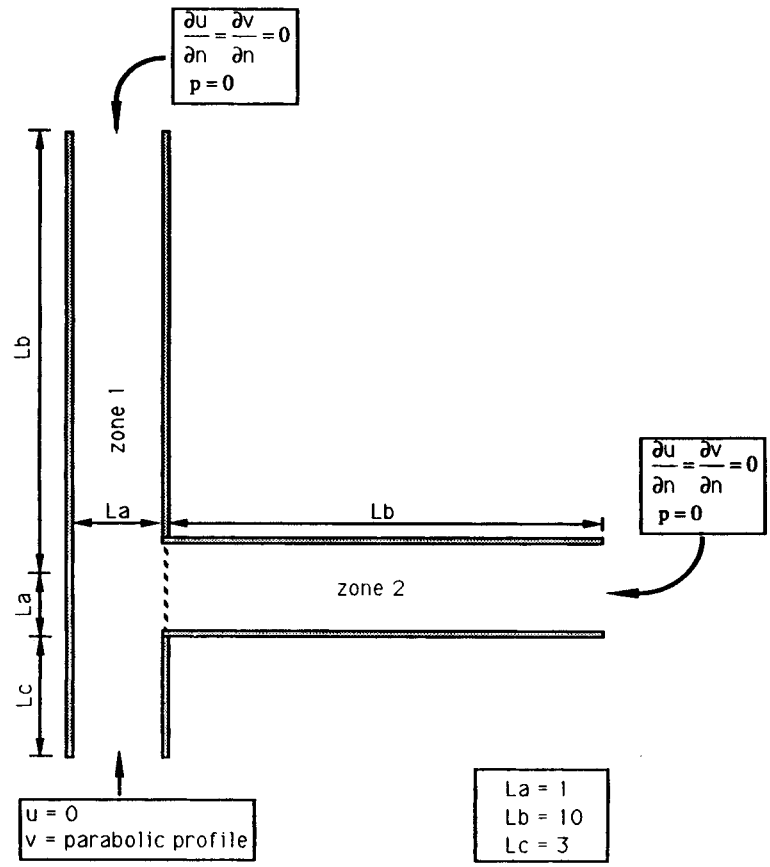

Figure 9. Description of 90° bifurcation problem. $La = 1{,}2$ $Lb = 10{,}2$ $Lc = 3$

10). Both formulations were based on the same streamline upwinding technique. The comparison demonstrates the differences in the pressure field that will result when higher-order pressure interpolation is used. The critical region of the flow path (upstream from the turn) is clearly different. The multi block approach prediction shows steeper gradients near the branch of the duct. The predicted recirculation zone lengths for these two cases did not differ by more than 2%.

4. CONCLUSIONS

A multiblock segregated equal-order finite element algorithm has been developed for the eight-noded element of the Serendipity family. This quadratic element was used primarily because it has a three-dimensional equivalent. Development of the basic algorithm and its extension into a multiblock approach are both provided. A number of validation test cases were selected and compared with existing experimental and analytical data. Perhaps the most promising finding of the current work is the total lack of discontinuities across the block interface boundaries for each of the different test cases. The analysis of the backward-facing step problem demonstrated the accuracy of the scheme through comparison with experimental data. The 90° bifurcation analysis showed that the current method is able to predict the correct physical trends for bifurcating flow. The study also showed the improvements in the pressure field that will result with a quadratic representation. It is believed that the

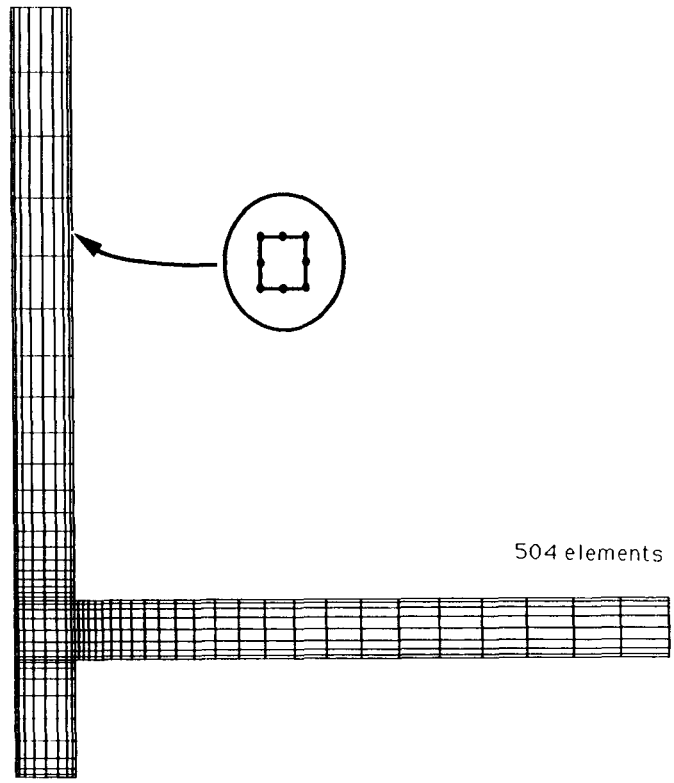

Figure 10. Composite finite element model of flow path

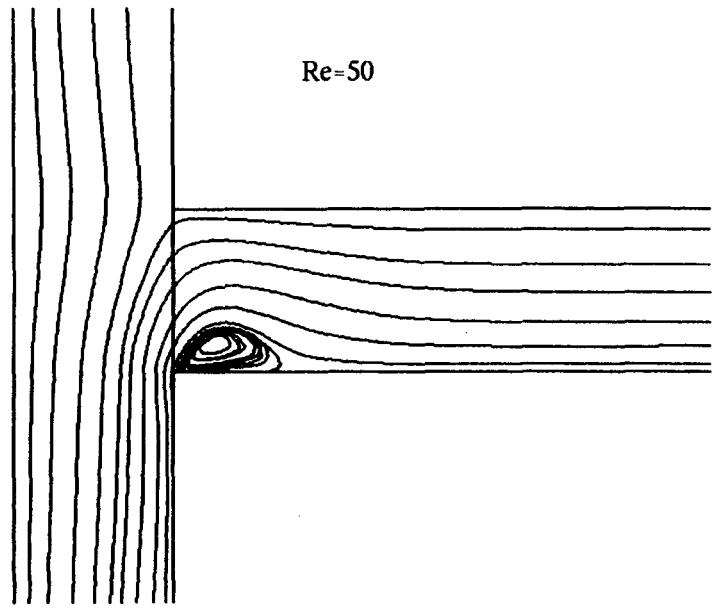

Figure 11. Streakline trace for Re = 50

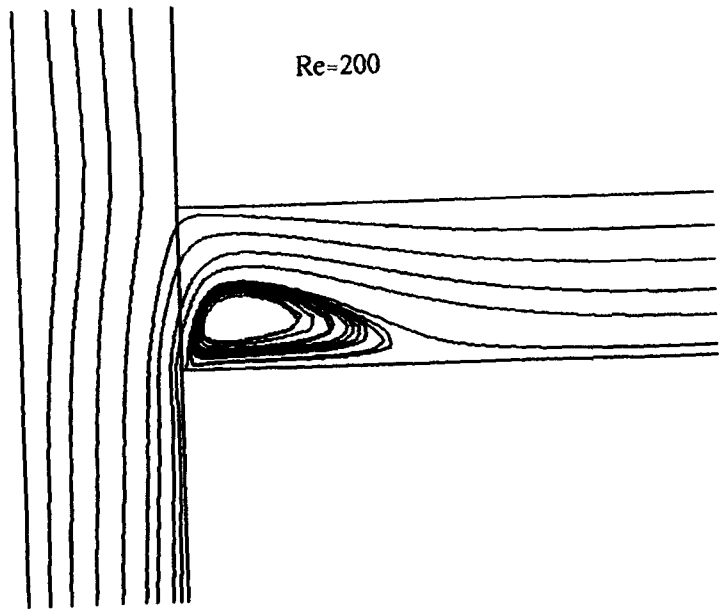

Figure 12. Streakline trace for $Re = 200$

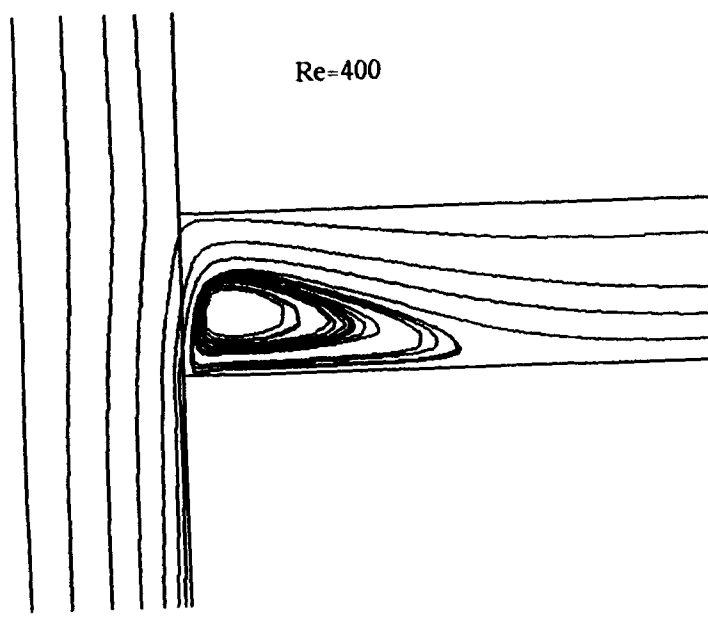

Figure 13. Streakline trace for $Re = 400$

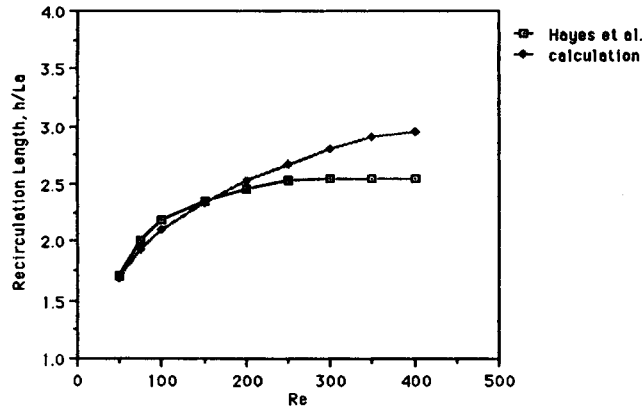

Figure 14. Variation in recirculation zone length with changing *Re*

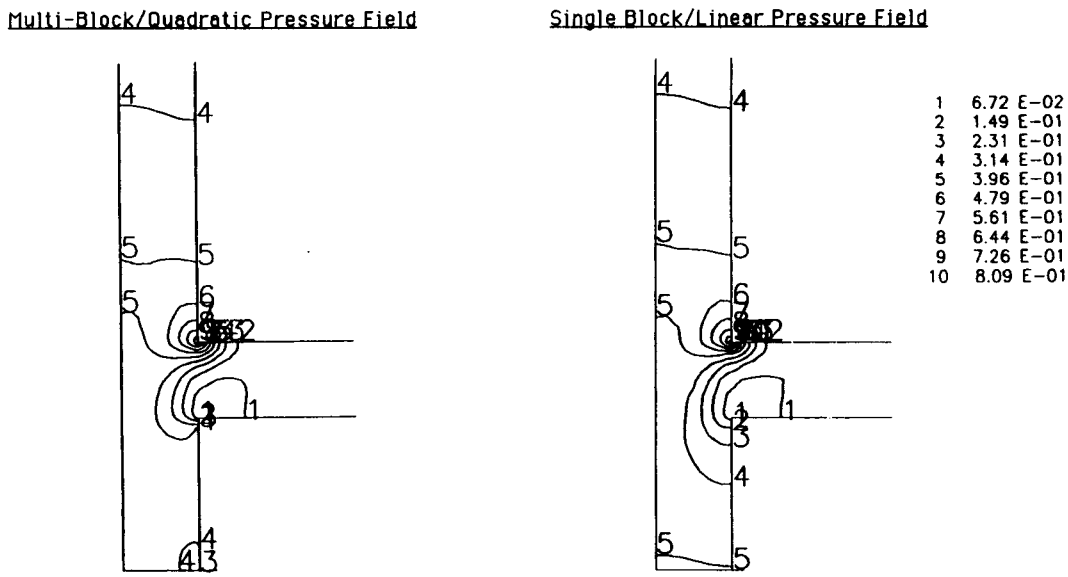

Figure 15. Comparison of pressure field for elements using quadratic and linear interpolation functions for pressure

proposed algorithm is the first true multiblock approach that does not use the 'patching' approximation of overlapping finite element blocks.

ACKNOWLEDGEMENT

This study was funded by the Turbomachinery Research Consortium, contract 32519-15190.

REFERENCES

1. W. M. Pun and D. B. Spalding, 'A general computer program for two-dimensional elliptic flows', *Rep. HTS/76/2*, Mechanical Engineering Department, Imperial College, London, 1976.
2. S. V. Patankar, *Numerical Heat Transfer and Fluid Flow*, Hemisphere, Washington, DC, 1980.
3. O. C. Zienkiewicz and R. L. Taylor, *The Finite Element Method*, Vol. 1, *Basic Formulation and Linear Problems*, 4th edn, McGraw-Hill, New York, 1988

4. M. L. James, G. M. Smith and J. C. Wolford, *Applied Numerical Methods for Digital Computation*, Harper and Row, New York, 1977.
5. A. C. Benim and W. Zinser, 'A segregated formulation of Navier–Stokes equations with finite elements', *Comput. Method Appl. Mech. Eng.*, **57**, 223–237 (1986).
6. O. C. Zienkiewicz, *The Finite Element Method*, McGraw-Hill, London, 1977.
7. K. H. Huebner and E. A. Thornton, *The Finite Element Method for Engineers*, Wiley, New York, 1982.
8. C. T. Shaw, 'Using a segregated finite element scheme to solve the incompressible Navier–Stokes equations', *Int. j. numer. methods fluids*, **12**, 81–92 (1991).
9. T. J. R. Hughes, 'A simple scheme for developing 'upwind' finite elements', *Int. j. numer. methods eng.*, **12** 1359–1365 (1978).
10. J. G. Rice and R. J. Schnipke, 'An equal-order velocity–pressure formulation that does not exhibit spurious pressure modes', *Comput. Methods Appl. Mech. Eng.*, 135–149 (1986).
11. J. G. Rice and R. J. Schnipke, 'A monotone streamline upwind finite element method for convection-dominated flows', *Comput. Method Appl. Mech. Eng.* 313–327 (1984).
12. C. A. J. Fletcher, *Computational Techniques for Fluids Dynamics*, Vol. 1, Springer, New York, 1991, Chap. 5.
13. L. Demkowicz, J. T. Oden and W. Rachowicz, 'A new finite element method for solving compressible Navier–Stokes equations based on an operator splitting method and h–p adaptivity', *Comput. Methods Appl. Mech. Eng.*, **84** 275–326 (1990).
14. R. Lohner, K. Morgan and O. C. Zienkiewicz, 'An adaptive finite element procedure for compressible high speed flows', *Comput. Methods Appl. Mech. Eng.*, **51**, 441–465 (1985).
15. J. Hetu and D. Pelletier, 'Adaptive remeshing for viscous incompressible flows', *AIAA J.*, **30**, 1986–1992 (1992).
16. R. Ramamurti and R. Lohner, 'A parallel implicit incompressible flow solver using unstructured meshes', *Naval Research Laboratory Rep. NRL/MR/6410-93-7178*, 1993.
17. F. M. White, *Viscous Fluid Flow*, McGraw-Hill, New York, 1974.
18. D. L. Hill and E. A. Baskharone, 'A monotone streamline upwind method for quadratic finite elements', *Int. j numer. methods fluids*, **17**, 463–475 (1993).
19. S. S. Rao, *The Finite Element Method in Engineering*, Pergamon, Oxford, 1989.
20. M. K. Denham and M. A. Patrick, 'Laminar flow over a downstream-facing step in a two dimensional flow channel', *Trans. Inst. Chem. Eng.*, **52**, 361–367 (1974).
21. O. C. Zienkiewicz, J. Szmelter and J. Peraire, 'Compressible and incompressible flow; an algorithm for all seasons', *Comput. Methods Appl. Mech. Eng.*, **78** 105–121 (1990).
22. R. E. Hayes, K. Nandakumar and H. Nasr-El-Din, 'Steady laminar flow in a 90 degree planar branch', *Comput. Fluids*, **17** 537–553 (1989).